Desalination and Water Treatment
www.deswater.com

doi: 10.5004/dwt.2022.28718

269 (2022) 132–140
September

Column adsorption study for the removal of phenol from aqueous medium using agro-residue adsorbent

Srihari Vedartham[a], Subramanyam Busetty[b,*], Ashutosh Das[c]

[a]*National Institute of Construction Management and Research (NICMAR), Hyderabad, India*
[b]*School of Civil Engineering, Centre for Bioenergy, SASTRA Deemed to be University, Thanjavur, Tamil Nadu, India – 613 401, emails: subramanyamjy@gmail.com/subramanyam@civil.sastra.edu*
[c]*Centre for Environmental Engineering, PRIST Deemed to be University, India*

Received 4 February 2022; Accepted 14 July 2022

ABSTRACT

In the wastewater treatment process, fixed-bed and packed bed studies on adsorption have become a popular technical application in industrial sector. In this work, the potential of activated carbon produced from black gram husk (BGH) for the removal of aqueous phenol in a fixed column was investigated. The study of breakthrough time and adsorption capacity augmented with an increase in bed height and minimized with an increase in rate of flow, initial concentration of phenol, and size of the particle. At best conditions of 10 cm height of bed, 100 mg/L as initial phenol concentration, 10 mL/min as flow rate and 300 μm is particle size and the breakthrough-curve of the lesser rate of flow (10 mL/min) increases sharply near the point of exhaustion, signifying that the zone of adsorption was squatter. The best rate of flow should not be greater than 10 mL/min. since the bed depth studied up to 14 cm, the minimum depth (D_{min}) was found to be 4 cm for a rate of flow of 10 mL/min. The time of breakthrough (T_b) vs bed depth [D] for bed depth service time plots were developed, and their comparisons of linear relationship were obtained with all correlation R^2 above 0.94. The capacity of adsorption (N_o) of BGH was considered to be 68.59 and 53.4 mg/cm^3 by using the rate of flow of 10 and 20 mL/min but N_o was sharply decreased to 30.57 mg/cm^3 with the rate of flow of 30 mL/min. The surface physical morphology of the adsorbents studied and the effect of adsorption, as explored by scanning electron microscopy micrographs showed increase in un-evenness of textures. In conclusion, our study has demonstrated that BGH can be utilized for successful removal of phenol from aqueous solutions. It was also shown that the modelling approach has a substantial impact on the outcome of dynamic adsorption system analysis.

Keywords: Phenol adsorption; Fixed-bed; Bed depth; Breakthrough time; Flow rate

1. Introduction

Phenol can be found in wastewater from a variety of chemical industries, including petrochemicals, paints, coal, oil refineries, leather, and medicines [1–5]. It can also be found in a variety of agricultural and household wastewaters [6–8]. Because of its toxicity, phenol is a serious contaminant. Even at low concentrations, it can induce a variety of ailments depending on the length of exposure [9]. It may come into contact with humans through mouthwash, creams, and other products. Due to various herbicides that influence the soil and groundwater, phenol is also present in agricultural run-off. Phenol lowers the porosity of soil, which affects seed germination. Because of seepage through the soil, it pollutes groundwater [10,11]. The Environmental Protection Agency (EPA) prohibits surface discharges with more than 1 part per million of phenol [12].

* Corresponding author.

Several methods for treating phenol-containing wastewater have been developed, including flocculation, oxidation, extraction, adsorption, reverse osmosis, enzyme degradation, ion exchange, and so on [13,14]. Adsorption has numerous benefits [15]. Activated carbon is a common adsorbent, but it is expensive [16,17]. In this regard, the production of activated carbon from renewable, readily available, and low-cost materials has been scrutinized [18]. Many scientists are now looking for alternative adsorbents in agricultural and industrial waste [19–23]. The detailed studies of phenol adsorption by various authors has presented in Table 1. The authors have carried out extensive study on various agro wastes and explored their adsorption capacities, kinetic and thermodynamic behavior [37].

Batch adsorption techniques may not be the most practical way to cope with high flow rates on an industrial scale. The adsorption process in a fixed-bed column study describes various advantages. First of all, it is continuous, and the adsorbent is continuously in contact with the adsorbate. Secondly it is low cost, simple and it can be developed for an industrial application. The main disadvantages are that there will be few separate routes can be formed in the column, which will enforce the short circuiting and hence the system of adsorption being irregular and bumpy so that design parameters may vary, which may affect the adsorption process. The adsorption process in a fixed-bed column system can be described by the numerical model [38], Artificial intelligence [39] and empirical models [40].

In this study, the efficacy of black gram husk (BGH) agro-waste in a continuous fixed-bed column for phenol removal was evaluated from various perspectives. This study also investigated significant commercial application difficulties such adsorbent regeneration, safe disposal of used adsorbents, and scale-up design. Mitra and Das [41], Mitra et al. [42], Singha et al. [43], Nag et al. [44–46], Banerjee et al. [47], Ghosh et al. [48], Mousumi et al. [49] have reported similar findings for metal and organic removal from aqueous solution.

The removal of organic material from aqueous solutions has been investigated using a variety of adsorbents. Activated carbon made from sawdust of *Tectona grandis* [50,51], activated carbon prepared from biomass material [52], coconut shell [53], rice husk and rice husk ash [54] has been proven to be effective at adsorbing organic compounds in studies. To goal of these investigations will aid in the acceptability of this research for a variety of industrial applications.

2. Methodology

2.1. Preparation of adsorbents

The proposed adsorbent (BGH) was rinsed thoroughly with water for the removal of dust and other soluble material and were kept to room temperature for drying. The dried agro-wastes were crumpled into fine powder and sieved through the standard sieves manually. The particles of I.S. sieve size 150–300 μ were collected, oven-dried (overnight, 105°C) desiccated and stored in air-tight containers for further studies [55].

2.2. Adsorbate for study

The analytical reagent (AR) grade phenol (C_6H_5OH) (Supplied by Ranbaxy Laboratories Ltd., India) was

Table 1
Detailed studies of phenol adsorption by various authors

S. No	Name of phenolic compound	Adsorbent	Adsorption capacity (mg/g)	References
1	Phenol	Activated carbon	140–256	[24]
		Apricot stone shell AC	120	[25]
		Tea leaves AC	438	[26]
		Bentonite	1.71	[27]
		Sawdust	146.25	[28]
		Fly ash	0.23–67	[29]
2	*p*-chlorophenol	Activated carbon	434	[30]
		Bentonite	10.63	[31]
		Perlite	5.84	[31]
3	2,4-dichlorophenol	Apricot stone shell AC	595	[25]
		Bituminous shale	4.2	[32]
4	2,3,4-trichlorophenol	Activated carbon	500	[33]
5	*m*-cresol	Apricot stone shell	113	[25]
		Fly ash	5.5	[34]
6	*o*-cresol	Palm seed coat	19.58	[35]
		Fly ash	3.1–4.7	[34]
7	Pyrogallol, pyrocatechol	Chemically treated sawdust	28–52	[36]
		Iron hydroxide coated marble	9–10	

utilized to prepare synthetic adsorbate solutions of various initial concentrations (C_o) in the choice of 10–100 mg/L. The necessary quantity of phenol was correctly weighed and mixed in distilled water phase-wise so as to made-up to 1 L in a measuring jar for further studies. The fresh phenol solution was prepared daily and preserved in a dark-coloured glass vessel of 5 L capacity, to avoid photo-oxidation. The initial concentration (C_o) was determined before the start of every experimental study. All experiments were carried out at least in duplicate.

2.3. Column studies

A column made up of glass with 30 cm length and internal diameter of 2.50 cm was used to contain the agro-based adsorbent as a fixed-bed adsorber. The column bed was maintained and closed by glass beads and glass wool, which confirm the flow of good liquid distribution. Then, distilled water was used to rinse the bed with and kept overnight to confirm a carefully filled preparation of particles without channels, voids, or cracks. The phenol solution was fed through a bed of agro-based packed adsorbent in the direction of up-flow to avoid channeling of the prepared solution. A pump with peristaltic principle was used to regulate the rate of flow at the entry and exit. The experimental samples of the solution were collected regularly and examined for the residual concentration of phenol (C_t) by using UV spectrophotometer. Therefore, the anticipated breakthrough for solution concentration (C_b) was evaluated at 10% of the entry feeder concentration (100 mg/L), which is proportionally equal to 0.1 C_t/C_o or 10 mg/L. The continuous flow through the prepared column was sustained until the concentration of phenol from column exit approached to 0.9 C_t/C_o, which specified as the exhaustion point (C_x). Now a curve was drawn between C_t/C_o vs. treated volume between the C_b and C_x, is called the breakthrough-curve.

2.4. Experimental studies on flow rate variable and bed depth

At three different flow rates of 10, 20, and 30 mL/min, the effects of flow rate and bed depth on column bed performance were examined at a constant bed depth. For studies, bed depths of 7, 10, and 14 cm were maintained. The standard column study parameter bed depth service time (BDST) curves were plotted between T_b and bed depth after the volume of breakthrough (V_b) and time of breakthrough (T_b) were determined (D). The relationship between T_b and D is given in the following equation using the Bohart–Adams model [56].

$$T_b = \frac{N_o D}{C_o V} - \frac{1}{KC_o} \ln\left(\frac{C_o}{C_b} - 1\right) \tag{1}$$

The straight-line equation of BDST curve is expressed as $y = mx + c$; where y = service time, x = bed depth, m = slope, and c = ordinate intercept. The value of the slope $m = N_o/C_oV$ and the intercept $c = \left(\frac{-1}{KC_o}\right)\left(\ln\left(\frac{C_o}{C_b} - 1\right)\right)$.

The system capacity of adsorption, N_o, and the rate constant, K, can be estimated from the slope of straight line and intercept of the straight line, respectively. The D_{min}, minimum bed depth can be estimated from the relationship by considering $T_b = 0$ and explaining for D [56].

2.5. Influence of rate of flow on breakthrough curve

The rate of flow determined by a standard parameter, the empty bed contact time (EBCT) in the given column study, which influence the volume of bed to breakthrough and the shape of breakthrough curve. The EBCT is calculated as:

$$\text{EBCT in min} = \frac{\text{Bed volume in cm}^3}{\text{Flow rate in } \frac{\text{cm}^3}{\text{min}}} \tag{2}$$

3. Fourier-transform infrared spectroscopy analysis

Alkanes, alkanols, alkyls, carboxylic acids, ethers, nitro compounds, and esters were detected in agro-waste activated carbon by Fourier-transform infrared spectroscopy (FTIR) analysis, while scanning electron microscopy (SEM) images confirmed the presence of interspatial holes within the matrix of the supplied adsorbent. Aside from porosity, the adsorption behaviour of activated carbon is influenced by the reactivity of chemical surfaces, particularly in the form of chemisorbed oxygen in various forms of functional groups. Both acidic and basic properties are present in surface oxides [57]. IR analysis enables for spectrophotometric monitoring of the adsorbent surface in the 400–4,000 cm^{-1} range, as well as direct identification of organic functional groups on the surface. An examination of the adsorbent surface before and after the adsorption reaction may reveal surface groups involved in the adsorption process, as well as the external spot(s) where adsorption may occur. Infrared studies reveal that specific functional groups participate in adsorption interactions.

3.1. SEM analysis

The SEM was a widely used essential tool for material classification ranging from nanometer to micrometer scale [58]. The surface structures are replicated in the image from SEM analysis. SEM explanations of various agricultural material samples obtained using a KYKY-2800 scanning electron microscope (CCM, Sherbrooke. Canada).

4. Results and discussion

4.1. Studies on designed column

In this study, Figs. 1–3 show the effect of selected three different flow rates on the study of breakthrough-curves by maintaining a bed depth of (a) 7 cm (b) 10 cm and (c) 14 cm, respectively. During the process, when the zone of adsorption moves up and the higher edge of this area spreads the top of the column, then the concentration of effluent starts to increase rapidly [59]. This point of

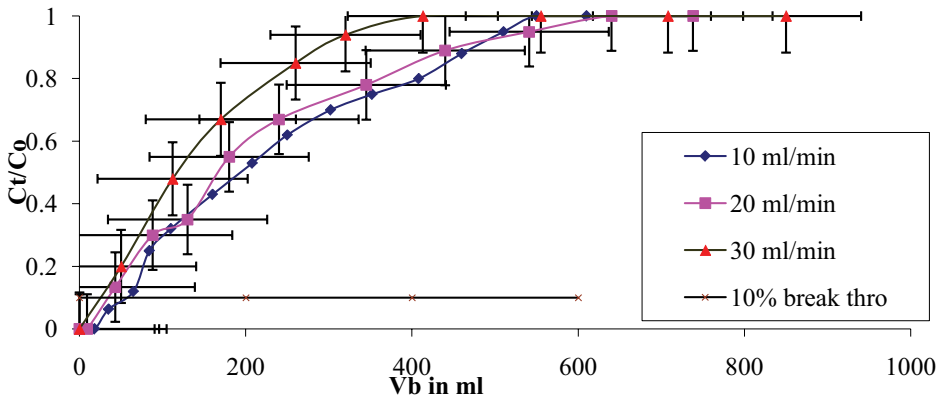

Fig. 1. Effect of flow rate on 7 cm depth with error bars represent the standard deviation.

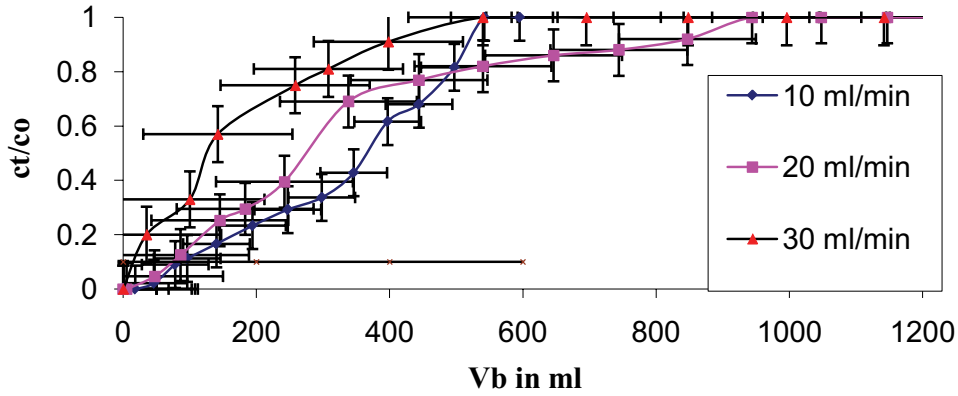

Fig. 2. Effect of flow rate on 10 cm depth with error bars represent the standard deviation.

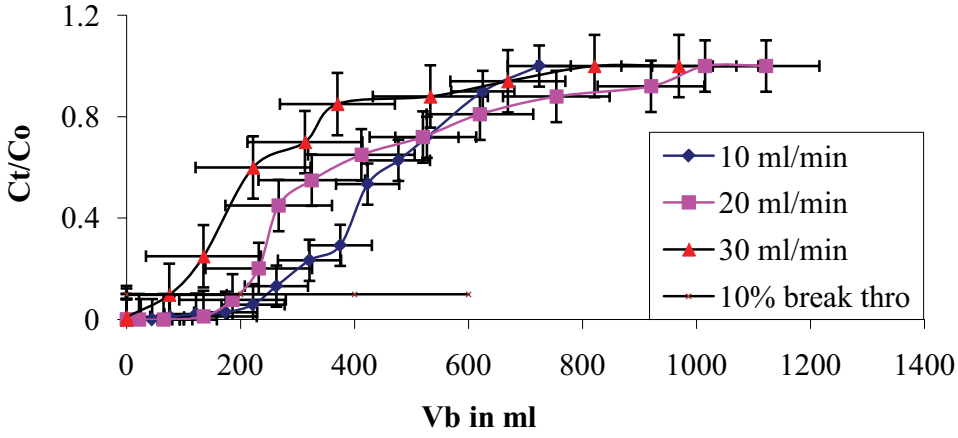

Fig. 3. Effect of flow rate on 14 cm depth with error bars represent the standard deviation.

rise is termed as the breakthrough point, corresponding volume of effluent collected indicated as V_b. The results reveal that the reduction in rate of flow at a standard bed depth raised the V_b and correspondingly the T_b, due to a raise in EBCT. Since the forward-facing adsorption zone touched the top of the designed glass column later by utilizing a gentler flow rate, more V_b was obtained.

The breakthrough-curve of the lesser rate of flow (10 mL/min) (Fig. 4) increases sharply near the point of exhaustion, signifying that the zone of adsorption was squatter, and the BGH as adsorbent was additionally saturated with the phenol [60,61]. Figs. 5 and 6 also show that the breakthrough-curve of 20 and 30 mL/min converted to less steep because the zone of adsorption was deeper.

The span of the zone of adsorption represents the smallest bed depth required to produce a low effluent phenol concentration when designing a glass column. This finding suggests that a lower flow rate or a longer contact time may be required for phenol adsorption by a column of BGH agro-waste adsorbent. The ideal flow rate for these study columns should be less than 10 mL/min to represent a shorter adsorption zone and a longer service time.

4.2. Influence of bed depth on breakthrough-curve

Figs. 4–6 describe the breakthrough curves of dissimilar bed depths at a persistent rate of flow of 10, 20 and 30 mL/min, respectively. The V_b or T_b improved with increasing bed depth while the shape and slope of the breakthrough-curves were marginally different with the variable bed depths.

However, the breakthrough-curves of the longer beds tend to be steadier, indicating that the designed column was difficult to completely exhaust. This result was complicated by using the upper rate of flow of 30 mL/min (Fig. 6). The rate of flow at the exit was uneven when the depth of bed was too high due to a greater flow obstruction caused by close packing of the longer bed packed with more BGH adsorbent. Although the raise in bed depth also increased the V_b or T_b, too large bed depth is not beneficial

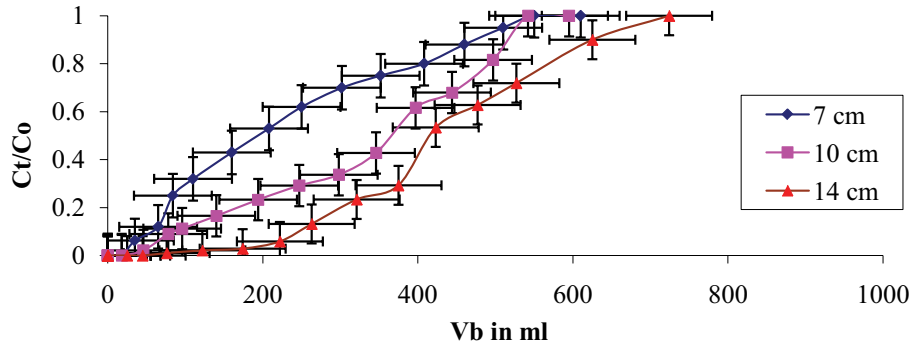

Fig. 4. Effect of bed depth for a flow rate of 10 mL/min with error bars represent the standard deviation.

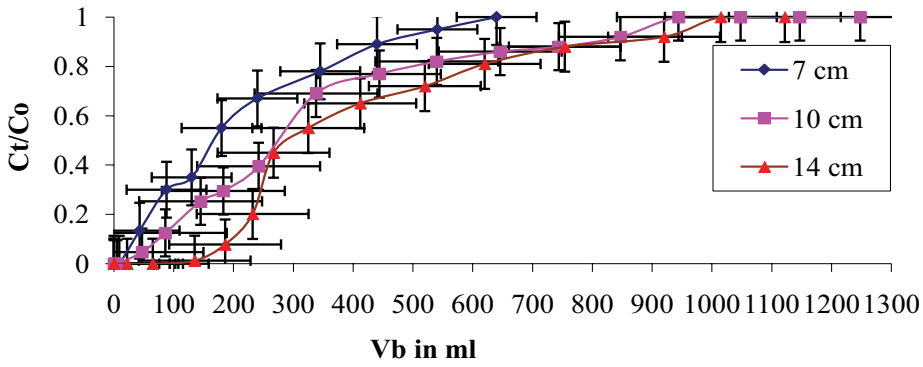

Fig. 5. Effect of bed depth for a flow rate of 20 mL/min.

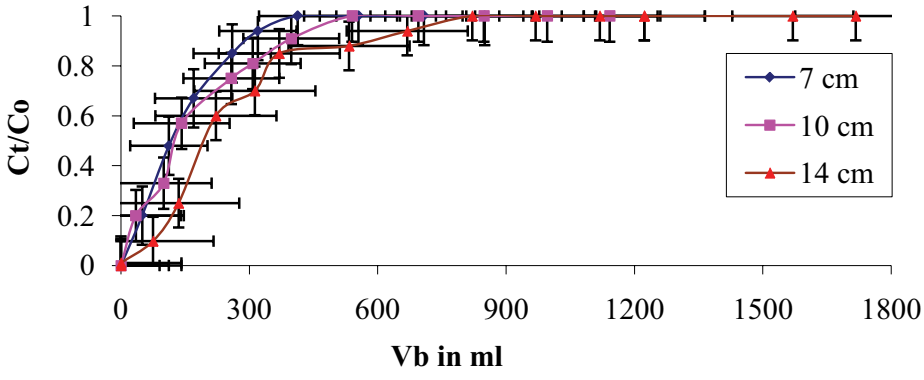

Fig. 6. Effect of bed depth for a flow rate of 30 mL/min with error bars represent the standard deviation.

for the study of single column; otherwise, the numerous beds should be developed. Since the treated phenol solution was not correctly drawn off at the upper portion of the packed-bed greater than 14 cm for the proportional diameter of 2.5 cm, the best depth to diameter ratio of designed column having BGH agro-based adsorbent should be lesser than 6 (<14/2.5). Actually, this proportion can be practical for the model prototype scale-up of the column adsorber.

4.3. Study of BDST with variation in depth of bed and rate of flow

The data of EBCT, V_b and T_b increased with decreasing flow rate or increasing bed depth. However, the flow rate of flow should not be reduced; it is determined by the detention period and the quantity of prepared phenol solution for treatment. As mentioned above, the bed depth should not be too high, therefore, the multiple beds arranged in parallel, or series are preferable. The T_b vs D for BDST plots were developed, which are shown in Figs. 7 and 8. The comparisons of linear relationship were obtained with all correlation R^2 above 0.94. Tables 2 and 3 shows the results of determining the minimum depth of bed (D_{min}), adsorption capacity (N_o), and rate constant (K). The results show that D_{min} increased as the rate of flow increased because the zone of adsorption must be improved to separate the wastewater sample, phenol, as the rate of flow increased. The real bed depth of black gram husk in the designed column of 2.5 cm diameter should be greater than 4.0, 4.48, and 4.98 cm, respectively, representing an appropriate length of phenol adsorption zone to achieve an acceptable effluent or to keep the phenol effluent concentration from exceeding 10 mg/L at null time test conditions. The capacity of adsorption (N_o) of BGH was estimated to be 68.59 and 53.4 mg/cm^3 when flow rates of flow of 10 and 20 mL/min were used, respectively, but N_o was sharply decreased to 30.57 mg/cm^3 when the rate of flow of 30 mL/min. This means that adsorption capacity can increase with decreasing rate.

4.4. Infrared characterization of individual agro-based adsorbents

As per the FTIR analysis, the spectrum for BGH (Fig. 9) exhibited the following bands. Noteworthy peak at –OH groups (3,449.36 cm^{-1}), –CH_2– group (2,924.06 cm^{-1}), C≡C bond (2,363.50 cm^{-1}), C=C bond (1,625.18 cm^{-1}), enlarging vibrations of aromatic C=C bonds, that is, phenyl (1,529.92 cm^{-1}), the syringyl ring with C–O enlarging (1,326.80 cm^{-1}), ethers with –C–O–C– stretches (1,017.02 cm^{-1}) and plane ring deformation, CH_2 rocking (667.14 cm^{-1}).

4.5. Influence of phenol-sorption on functional groups of the adsorbents

The influence of adsorption reaction of phenolic adsorbate over the BGH carbon studied has resulted in some

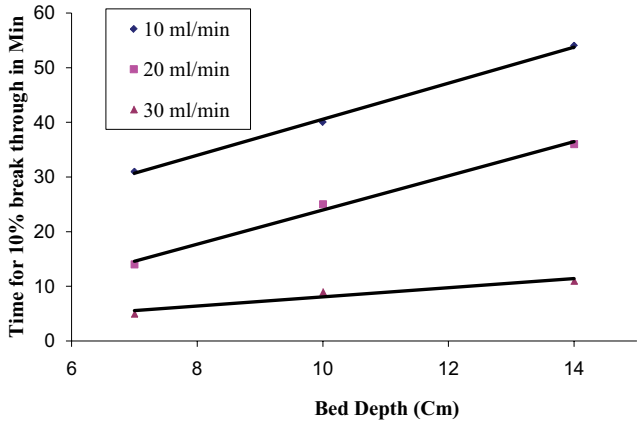

Fig. 7. BDST curves for 10% breakthrough.

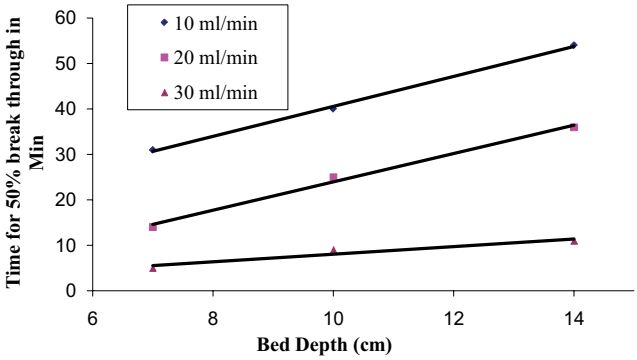

Fig. 8. BDST curves for 50% breakthrough.

Table 2
Details of bed depth and rate of flow in fixed-bed column

Q (mL/min)	D (cm)	Bed volume (cm^3)	EBCT (min)	V_b (mL)	T_b (10%) min
10	7	34.34	3.43	55	9
	10	49.06	4.9	88	13
	14	68.68	6.8	240	32
20	7	34.34	1.71	23	4
	10	49.06	2.45	27	6
	14	68.68	3.43	205	13
30	7	34.34	1.14	8	1.5
	10	49.06	1.63	50	3
	14	68.68	2.28	112	5

Table 3
Constants of BDST equations

Q (mL/min)	V (cm/min)	D_{min} (cm)	N_o (mg/L)	K (L/mg × 10^{-3})
10	2.04	4.0	68.59	1.31
20	4.08	4.48	53.4	3.74
30	6.12	4.98	30.57	10.98

unusual changes such as the disappearance of some special changes such as vanishing of some bands, the enlargement of others, and spectral shifts. The peculiar changes in the spectra of the phenol unloaded and loaded adsorbents are due to variations in the surface characteristics, such as the contribution of specific functional groups in the principle of adsorption interaction and resulting chemical variations thereon. The BGH carbon's crests at 3,449.36 cm^{-1} vanished, and a broad band around 3,000–3,500 cm^{-1} appeared for the phenolic adsorbate loaded carbons, indicating the participation of phenolic groups in the adsorption reaction. Figs. 9 and 10 depict typical FTIR bands. The enlarging vibrations of aromatic C=C bonds (i.e., phenyl) are explained by the peaks at 1,625 and 1,529 cm^{-1} [62,63]. The sharp peak variations between 1,326 and 1,230 cm^{-1} indicate the formation of the syringyl ring via C–O stretching. Peak shifts from 1017 to 1012 correspond to ether stretches –C–O–C. The plane ring deformation is described by the peak of 667–668 [64].

The increase in –OH groups on BGH (Fig. 9) was found to be 3.6%. After adsorption, the effect of $–CH_2–$ groups decreases by 8%, as demonstrated by BGH. At wavelengths of 1,734; 1,500–1,600 and 1,461 cm^{-1}, the effect of phenol uptake on the surface reduces C=O stretching, aromatic C=C bond, and methyl ($–CH_3$) group in all types of adsorbents. Simultaneously, C–O stretch or –OH distortion in carboxylic acids (1,425 cm^{-1}); $–CH_3$ distortion (1,376 cm^{-1}): syringyl ring with C–O elongating (1,329 cm^{-1}) and C–O stretches (1,247 cm^{-1}) [66]; ethers –C–O–C– stretches (1,050 cm^{-1}); C–H out of plane deformation (897 cm^{-1}); C–H out of plane bending in benzene derivatives (853 cm^{-1}) and in-plane bending in benzene derivatives (853 cm^{-1}) and in-plane ring distortion (608 cm^{-1}) also shows the decrease of their proportion [64].

4.6. SEM analysis of adsorbents

SEM studies are widely used to understand the morphological features and textural characteristics of the adsorbent (here BGH) materials [48,49]. In the present study, SEM procedure was engaged to perceive the textural physical morphology, that is, texture of surface and porosity of the agro-based BGH adsorbents at the best operational condition with 2,000× magnifications. It can be visualized from the micrographs that the outer surface of the chemically acidulated adsorbent is full of alterations and striations with cavities.

It appears that the cavities caused by acidification and carbonization induce agglomeration on the carbonise structure, which is further revealed in the formation of chars with a complete exterior surface. There are some scatterings

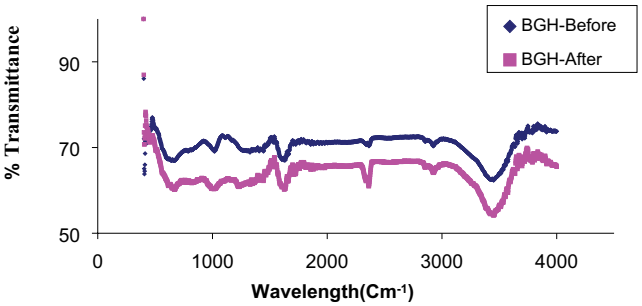

Fig. 9. Comparison of FTIR analysis of BGH before and after adsorption.

visible on the surface of the BGH adsorbents (as well as, to some extent, some blockage of the entry of pores). The findings above clearly show that the products' adsorptive capacity can be increased further.

In some adsorbents the surface was also found to be covered with several spherical silica elements that contain sharp, conical agglomerations [65]. It was also observed that a solidifying of the basal cell forming a surrounding brim with attendant depressions allowing the adsorbent surface to accommodate the silica bodies. Moreover, the silica globules appeared to be more visible due to the leveling off or reduction of the thick basal cell brim. The dense surface was found to be transformed to uneven textures and layers. The presence of small pores on most of the adsorbed adsorbents' surface showed the possible development of rudimentary pore networks.

The image of BGH displays a heterogeneous surface (with several macropores) as seen from its SEM micrographs (Figs. 10 and 11). BGH seems to possess a characteristic cellulose-morphology (with twisted strands), possibly exposed due to pre-treatment and adsorption. The consequence of pretreatment and adsorption seemed to result in increased number and size of voids, akin to that of char-based carbons.

5. Conclusions

In a column investigation, BGH agro-waste was found to be capable of dephenolation from aqueous phenolated solution to a degree comparable to commercial activated carbon, but at a significantly lower cost. The design parameters bed depth and flow rate for an adsorption bed were determined based on column studies. The optimal rate of flow is less than 10 mL/min, and with a rate of flow of 10 mL/min, the D_{min} was determined to be 4 cm for a bed depth of up to 14 cm. In terms of agro-wastes

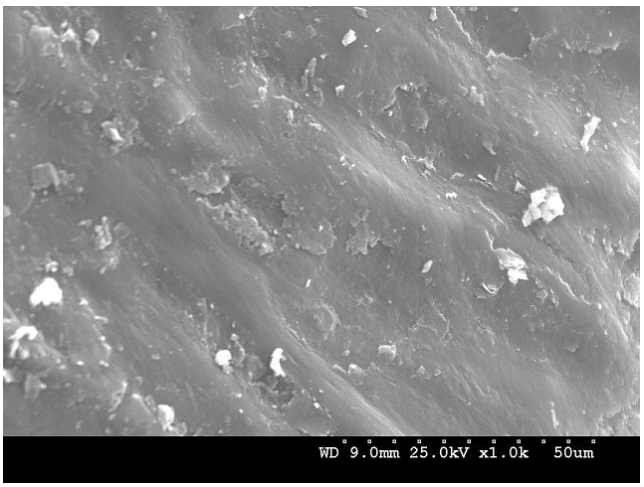

Fig. 10. SEM analysis of BGH before treatment.

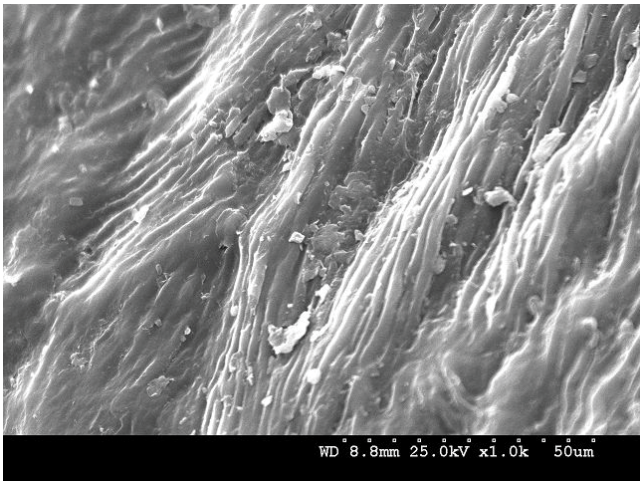

Fig. 11. SEM analysis of BGH treatment.

characterization, the FTIR record reveals the existence of numerous functional groups in these samples, including lactones, phenols, ethers, and carboxyl. The FTIR examination of the adsorbent before and after adsorption reveals unique spectrum alterations of band disappearance and spectral shifts is expansions. Adsorption causes changes in aromatic C=C, C–O, and aliphatic (–CH_3 and –CH_2) functional groups, as well as changes in the peaks of –C–O–C bonds, adsorbent-specific fluctuations in the –OH group, and so on. SEM micrographs of the adsorbent's surface physical morphology revealed an increase in texture un-evenness, the development of alterations and striations with cavities on the outer surface of the chemically acidulated and carbonised adsorbents, and the exposure of the silica globules due to the shrinkage of the thick basal cell brims.

Acknowledgement

The authors acknowledge Dept. of Science and Technology (DST): SUTRAM FOR EASY WATER (DST/TM/WTI/WIC/2K17/82(G)) for financial support for carrying out this research.

References

[1] O.J. Hao, H. Kim, P.-C. Chiang, Decolorization of wastewater, Crit. Rev. Env. Sci. Technol., 30 (2000) 449–505.
[2] F.A. Banat, B. Al-Bashir, S. Al-Asheh, O. Hayajneh, Adsorption of phenol by bentonite, Environ. Pollut., 107 (2000) 391–398.
[3] A. Mandal, S.K. Das, Phenol adsorption from wastewater using clarified sludge from basic oxygen furnace, J. Environ. Chem. Eng., 7 (2019) 103259, doi: 10.1016/j.jece.2019.103259.
[4] Sheets Fact, Breast Cancer and The Environment Research Centers, 2007.
[5] A. Mandal, S.K. Das, Adsorptive removal of phenol by activated alumina and activated carbon from coconut coir and rice husk ash, Water Conserv. Sci. Eng., 4 (2019b) 149–161.
[6] A. Mandal, P. Mukhopadhyay, S.K. Das, Removal of phenol from aqueous solution using activated carbon from coconut coir, IOSR J. Eng., 8 (2018) 41–55.
[7] A. Mandal, P. Mukhopadhyay, S.K. Das, The study of adsorption efficiency of rice husk ash for removal of phenol from wastewater with low initial phenol concentration, SN Appl. Sci., 1 (2019a) 192–204.
[8] A. Mandal, P. Mukhopadhyay, S.K. Das, Efficiency analysis of rice husk as adsorbent for removal of phenol from wastewater, J. Environ. Anal. Toxicol., 9 (2019b) 605–612.
[9] Z. Aksu, J.A. Yener, A comparative adsorption/biosorption study of mono-chlorinated phenol onto various sorbent, Waste Manage., 21 (2001) 695–702.
[10] S. Lakshmi, M. Harshitha, G. Vaishali, S.R. Keerthana, R. Muthappa, Studies on different methods for removal of phenol in wastewater, Int. J. Sci. Eng. Technol. Res., 5 (2016) 2488–2496.
[11] M.T. Uddin, M.S. Islam, A.Z. Abedin, Adsorption of phenol from aqueous solution by water hyacinth ash, ARPN J. Eng. Appl. Sci., 2 (2007) 11–17.
[12] N.N. Dutta, S. Borthakur, G.S. Patil, Phase transfer catalyzed extraction of phenolic substances from aqueous alkaline stream, Sep. Sci. Technol., 27 (2006) 1435–1448.
[13] S.H. Lin, R.S. Juang, Adsorption of phenol and its derivatives from water using synthetic resins and low-cost natural adsorbents: a review, J. Environ. Manage., 90 (2009) 1336–1349.
[14] L.G.C. Villegas, N. Mashhadi, M. Chen, D. Mukherjee, K.E. Taylor, N. Biswas, A short review of techniques for phenol removal from wastewater, Curr. Pollut. Rep., 2 (2016) 157–167.
[15] G.S. Garbellini, G.R. Salazar-Banda, L.A. Avaca, Effects of ultrasound on the degradation of pentachlorophenol by boron-doped diamond electrodes, Port. Electrochim. Acta, 28 (2010) 405–415.
[16] H. Lalhruaitluanga, K. Jayaram, M.N.V. Prasad, K.K. Kumar, Lead(II) adsorption from aqueous solutions by raw and activated charcoals of *Melocanna baccifera* Roxburgh (bamboo)—a comparative study, J. Hazard. Mater., 175 (2010) 311–318.
[17] A.H. Al-Muhtaseb, K.A. Ibrahim, A.B. Albadarin, O. Al-ikhashman, G.M. Walker, M.N. Ahmad, Remediation of phenol-contaminated water by adsorption using poly methyl methacrylate, Chem. Eng. J., 168 (2011) 691–699.
[18] M.J. Amiri, R. Roohi, M. Arshadi, A. Abbaspourrad, 2,4-D adsorption from agricultural subsurface drainage by canola stalk-derived activated carbon: insight into the adsorption kinetics models under batch and column conditions, Environ. Sci. Pollut. Res., 27 (2020) 16983–16997.
[19] A. Dabrowski, P. Podkoscielny, M. Hubicki, M. Barczak, Adsorption of phenolic compounds by activated carbon – a critical review, Chemosphere, 58 (2005) 1049–1070.
[20] S.-H. Lin, R.-S. Juang, Adsorption of phenol and its derivatives from water using synthetic resins and low-cost natural adsorbents: a review, J. Environ. Manage., 90 (2009) 1336–1349.
[21] A. Gundogdu, C. Duran, H.B. Senturk, M. Soylak, D. Ozdes, H. Serencam, M. Imamoglu, Adsorption of phenol from aqueous solution on a low-cost activated carbon produced from tea industry waste: equilibrium, kinetics, and thermodynamic study, J. Chem. Eng. Data, 57 (2012) 2733–2743.

[22] H.A. Asmaly, I.B. Abussaud, T.A. Saleh, T. Laoui, V.K. Gupta, M.A. Atieh, Adsorption of phenol on aluminium oxide impregnated fly ash, Desal. Water Treat., 57 (2015) 6801–6808.
[23] S. Sarkar, S.K. Das, Removal of hexavalent chromium from aqueous solution using natural adsorbents – column studies, Int. J. Eng. Res. Technol., 5 (2016) 370–377.
[24] V.C. Srivastava, M.M. Swamy, I.D. Mall, B. Prasad, I.M. Mishra, Adsorptive removal of phenol by bagasse fly ash and activated carbon: equilibrium, kinetics, and thermodynamics, Colloids Surf., A, 272 (2006) 89–104.
[25] A.A.M. Daifullah, B.S. Girgis, Removal of some substituted phenols by activated carbon obtained from agricultural waste, Water Res., 32 (1998) 1169–1177.
[26] D.K. Singh, B. Srivastava, Removal of some phenols by activated carbon developed from used tea leaves, J. Ind. Pollut. Control, 16 (2000) 19–30.
[27] B. Xie, J. Qin, S. Wang, X. Li, H. Sun, W. Chen, Adsorption of phenol on commercial activated carbons: modelling and interpretation, Int. J. Environ. Res. Public Health, 17 (2020) 789.
[28] D.N. Jadhav, A.K. Vanjara, Adsorption equilibrium study: removal of dyestuff effluent using sawdust, polymerized sawdust and sawdust carbon-I, Indian J. Chem. Technol., 11 (2004) 194–200.
[29] E. Haribabu, Y.D. Upadhya, S.N. Upadhyay, Removal of phenols from effluents by fly ash, Int. J. Environ. Stud., 43 (1993) 169–176.
[30] G. McKay, M.J. Bino, A.R. Altamemi, The adsorption of various pollutants from aqueous solutions on to activated carbon, Water Res., 19 (1985) 491–495.
[31] B. Koumanova, P. Peeva-Antova, Adsorption of *p*-chlorophenol from aqueous solutions on bentonite and perlite, J. Hazard. Mater., 90 (2002) 229–234.
[32] E. Tutem, R. Apak, C.F. Unal, Adsorptive removal of chlorophenols from water by bituminous shale, Water Res., 32 (1998) 2315–2324.
[33] K. László, A. Bóta, L.G. Nagyu, Characterization of activated carbons from waste materials by adsorption from aqueous solutions, Carbon, 35 (1997) 593–598.
[34] Kr. B. Singh, N.S. Rawat, Comparative sorption equilibrium studies of toxic phenols on fly ash and impregnated fly ash, J. Chem. Technol. Biotechnol., 61 (1994) 307–317.
[35] S. Rengaraj, R. Sivabalan, B. Arabindoo, V. Murugesan, Adsorption kinetics of *o*-cresol on activated carbon from palm seed coat, Indian J. Chem. Technol., 7 (2000) 127–131.
[36] D.K. Sing, A. Mishra, Removal of organic pollutants by the use of iron(III) hydroxide-loaded marble, Sep. Sci. Technol., 28 (1993) 1923–1931.
[37] V. Srihari, A. Das, The kinetic and thermodynamic studies of phenol-sorption onto three agro-based carbons, Desalination, 225 (2008) 220–234.
[38] M.J. Amiri, R. Roohi, A. Gil, Numerical simulation of Cd(II) removal by ostrich bone ash supported nanoscale zero-valent iron in a fixed-bed column system: utilization of unsteady advection-dispersion-adsorption equation, J. Water Process Eng., 25 (2018) 1–14.
[39] M.J. Amiri, M. Khozaei, A. Gil, Modification of the Thomas model for predicting unsymmetrical breakthrough curves using an adaptive neural-based fuzzy inference system, J. Water Health, 17 (2019) 25–36.
[40] M. Bahrami, M.J. Amiri, B. Beigzadeh, Adsorption of 2,4-dichlorophenoxyacetic acid using rice husk biochar, granular activated carbon, and multi-walled carbon nanotubes in a fixed-bed column system, Water Sci. Technol., 78 (2018) 1812–1821.
[41] T. Mitra, S.K. Das, Cr(VI) removal from aqueous solution using *Psidium guajava* leaves as green adsorbent: column studies, Appl. Water Sci., 9 (2019) 153, doi: 10.1007/s13201-019-1029-2.
[42] T. Mitra, N. Bar, S.K. Das, Rice husk: green adsorbent for Pb(II) and Cr(VI) removal from aqueous solution–column study and GA–NN modeling, SN Appl. Sci., 1 (2019) 486, doi: 10.1007/s42452-019-0513-5.
[43] B. Singha, N. Bar, S.K. Das, The use of artificial neural network (ANN) for modeling of Pb(II) adsorption in batch process, J. Mol. Liq., 211 (2015) 228–232.
[44] S. Nag, A. Mondal, N. Bar, S.K. Das, Bio-sorption of chromium(VI) from aqueous solutions and ANN modeling, Environ. Sci. Pollut. Res., 24 (2017) 18817–18835.
[45] S. Nag, A. Mondal, D.N. Roy, N. Bar, S.K. Das, Sustainable bioremediation of Cd(II) from aqueous solution using natural waste materials: kinetics, equilibrium, thermodynamics, toxicity studies and GA-ANN hybrid modelling, Environ. Technol. Innovation, 11 (2018) 83–104.
[46] S. Nag, N. Bar, S.K. Das, Sustainable bioremediation of Cd(II) in fixed-bed column using green adsorbents: application of kinetic models and GA-ANN technique, Environ. Technol. Innovation, 13 (2019) 130–145.
[47] M. Banerjee, B. Ranjan Kumar, D. Sudip Kumar, Cr(VI) adsorption by a green adsorbent walnut shell: adsorption studies, regeneration studies, scale-up design and economic feasibility, Process Saf. Environ. Prot., 116 (2018b) 693–702.
[48] K. Ghosh, B. Nirjhar, B. Asit Baran, D. Sudip Kumar, Removal of methylene blue (aq) using untreated and acid-treated eucalyptus leaves and GA-ANN modelling, Can. J. Chem. Eng., 97 (2019) 2883–2898.
[49] B. Mousumi, K. Arun Guha, R. Lalitagauri, Adsorption of lead on lentil husk in fixed-bed column bioreactor, Bioresour. Technol., 283 (2019) 86–95.
[50] E.I. Unuabonah, B.I. Olu-Owolabi, E.I. Fasuyi, K.O. Adebowale, Modeling of fixed-bed column studies for the adsorption of cadmium onto novel polymer–clay composite adsorbent, J. Hazard. Mater., 179 (2010) 415–423.
[51] K. Mohanty, D. Das, M.N. Biswas, Adsorption of phenol from aqueous solutions using activated carbons prepared from *Tectona grandis* sawdust by $ZnCl_2$ activation, Chem. Eng. J., 115 (2005) 121–131.
[52] B.H. Hameed, A.A. Rahman, Removal of phenol from aqueous solutions by adsorption onto activated carbon prepared from biomass material, J. Hazard. Mater., 160 (2008) 576–581.
[53] A.T. Mohd Din, B.H. Hameed, A.L. Ahmad, Batch adsorption of phenol onto physiochemical-activated coconut shell, J. Hazard. Mater., 161 (2009) 1521–1529.
[54] A.H. Mahvi, A. Maleki, A. Eslami, Potential of rice husk and rice husk ash for phenol removal in aqueous systems, Am. J. Appl. Sci., 1 (2004) 321–326.
[55] V. Srihari, A. Das, Comparative studies on adsorptive removal of phenol by three agro-based carbons: equilibrium and isotherm studies, Ecotoxicol. Environ. Saf., 71 (2008) 274–283.
[56] B. Volesky, I. Prasetyo, Cadmium removal in bio-sorption column, Biotechnol. Bioeng., 43 (1994) 1010–1015.
[57] V. Gómez-Serrano, F. Piriz-Almeida, C.J. Duran-Valle, J. Pastor-Villegas, Formation of oxygen structures by air activation. A study by FT-IR spectroscopy, Carbon, 37 (1999) 1517–1528.
[58] I. Ghosh, S. Kar, T. Chatterjee, N. Bar, S.K. Das, Adsorptive removal of Safranin-O dye from aqueous medium using coconut coir and its acid-treated forms: adsorption study, scale-up design, MPR and GA-ANN modelling, Sustainable Chem. Pharm., 19 (2021) 100374, doi: 10.1016/j.scp.2021.100374.
[59] S.D. Faust, O.M. Aly, Adsorption Process for Water Treatment, Butterworths Publishers, Stoneham, 1987.
[60] W.W. Eckenfelder, Industrial Water Pollution Control, 3rd ed., McGraw-Hill International, Boston, 2000.
[61] L.D. Benefield, J.F. Judkins, B.L. Weand, Process Chemistry for Water and Wastewater Treatment, Prentice-Hall, Englewood Cliffs, 1982, p. 212.
[62] C.A. Lua, J. Guo, Chars pyrolyzed from oil palm wastes for activated carbon preparation, J. Environ. Eng., 125 (1999) 72–76.
[63] H.P. Boehm, Surface oxides on carbon and their analysis: a critical assessment, Carbon, 40 (2002) 145–149.
[64] A. Mandal, N. Bar, S.K. Das, Phenol removal from wastewater using low-cost natural bio-adsorbent neem (*Azadirachta indica*) leaves: adsorption study and MLR modeling, Sustainable Chem. Pharm., 17 (2020) 100308, doi: 10.1016/j.scp.2020.100308.
[65] J.W. Nelly, E.G. Isacoff, Carbonaceous Adsorbents for the Treatment of Ground and Surface Water, Marcel Dekker, New York, 1982.
[66] J.J. Rook, Treatment of Water by Granular Activated Carbon, M.J. McGuire, I.H. Suffet, Ed., American Chemical Society, Washington, D.C., 1983.